CLOUD IDENTIFICATION AND OPTICAL THICKNESS RETRIEVAL USING AVIRIS DATA

Kwo-Sen Kuo, Ronald M. Welch, Institute of Atmospheric Science, South Dakota School of Mines and Technology, Rapid City, South Dakota, USA; Bo-Cai Gao, Alexander F. H. Goetz, Center for the Study of Earth from Space/Cooperative Institute for Research in Environmental Sciences, University of Colorado, Boulder, Colorado, USA.

ABSTRACT

An improved ratioing technique is introduced for cloud identification. Optical thicknesses for cloudy areas are obtained using albedos calculated by a radiative transfer model at 0.752 μm. A comparison of the optical thickness results from images of different resolutions is then made to demonstrate the need of high resolution data for cloud property retrievals.

INTRODUCTION

Understanding the role of clouds is among the highest priorities in the EOS (Earth Observing System) science objectives. In order to fully understand the formation and feedback processes of clouds, an accurate measurement of their microphysical properties is necessary. Remotely sensed data by satellites provide a means to monitor clouds globally, and hence the ability to assess the geographical effects on cloud formation and composition. Therefore retrieval algorithms of cloud properties using satellite data are highly in demand.

In this report we will discuss an improved technique in cloud identification and a preliminary study on retrieving cloud optical thickness using AVIRIS data.

DATA

AVIRIS is the prototype of the proposed HIRIS instrument for the EOS project. A brief description of the AVIRIS instrument and data can be found in Gao and Goetz (1990b). Each AVIRIS scene usually has 512 scan lines with 614 pixels per line and 224 channels per pixel. The pixel ground resolution is about 20 x 20 meters square. Each pixel is represented by a 2-byte integer on magnetic tape and is readily converted to radiance by multiplying a conversion factor. In this study we further converted radiance to albedo using solar zenith angle and solar irradiance calculated by a LOWTRAN7

model for each channel. A subset (600 x 480 pixels) of the full scene is used for the convenience of spatial degradation.

CLOUD IDENTIFICATION

The identification of clouds in an image is the first step and also a major difficulty in cloud property retrieval using remotely sensed imagery. Almost every existing cloud identification algorithm involves a choice of threshold. Such choice is often more or less subjective. Therefore the results of a cloud property analysis derived from different cloud identification algorithms can possess a large range of variability (Parker and Wielicki, 1989).

Gao and Goetz (1990a) developed a technique which enables one to make a distinction between cloud and background with greater confidence. For each AVIRIS image pixel they first take the five-channel averaged radiance over the water vapor absorption channels centered at 0.94 and 1.14 μm respectively, and over the window channels between them centered at 1.04 μm. The ratio of the sum radiance from the two averaged water vapor channels to twice the radiance of the averaged window channel is then taken for each pixel. (This process will be referred to as 3-band ratioing and the ratio obtained from this process as 3-band ratio, hereafter.) And a ratioed image is thus generated after a linear contrast stretch to put pixel ratios in integers for storage and display purposes.

In the ratioed image, clouds stand out from a rather uniform background over land. (See Gao and Goetz, 1990a, for examples.) This is because most soil ingredients have a linear spectral response in this wavelength region (Gao and Goetz, 1990b). However, where there is an uneven terrain it will show a brightness gradient on the ratioed image, because higher terrains cause shorter water absorption paths hence less water absorption and larger ratios. This effect somewhat obscures the distinction between cloud and background and makes the choice of threshold more difficult than on an even terrain. It is desirable to be able to improve this technique in this regard.

Figure 1 shows the histograms from the three averaged channels of AVIRIS scene AS0628. The three-maximum characteristics of the histograms are very typical for an image composed of shadows cast by clouds, background features, and a good portion of clouds. These histograms can be viewed as composites of the distributions of three classes of pixels (Fig. 2) with the maximum of the lowest albedo corresponding to the distribution of shadow pixels, and similarly the second maximum to the background pixels and the third to cloudy pixels.

With closer examination we found that water vapor absorption poses two effects to the histograms: (1) narrowing the distribution of each class, and (2)

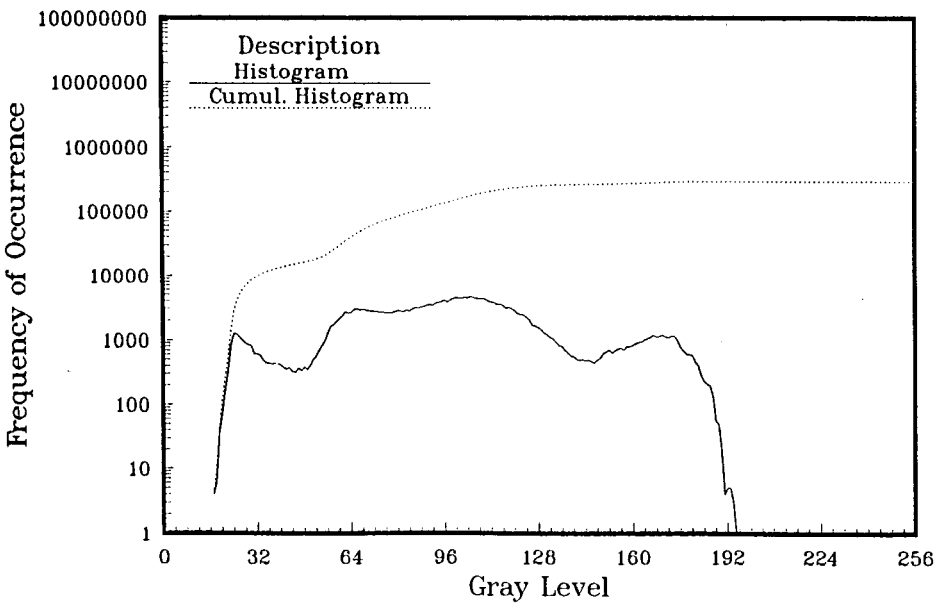

Figure 1a. Window channel centered at 1.04 μm.

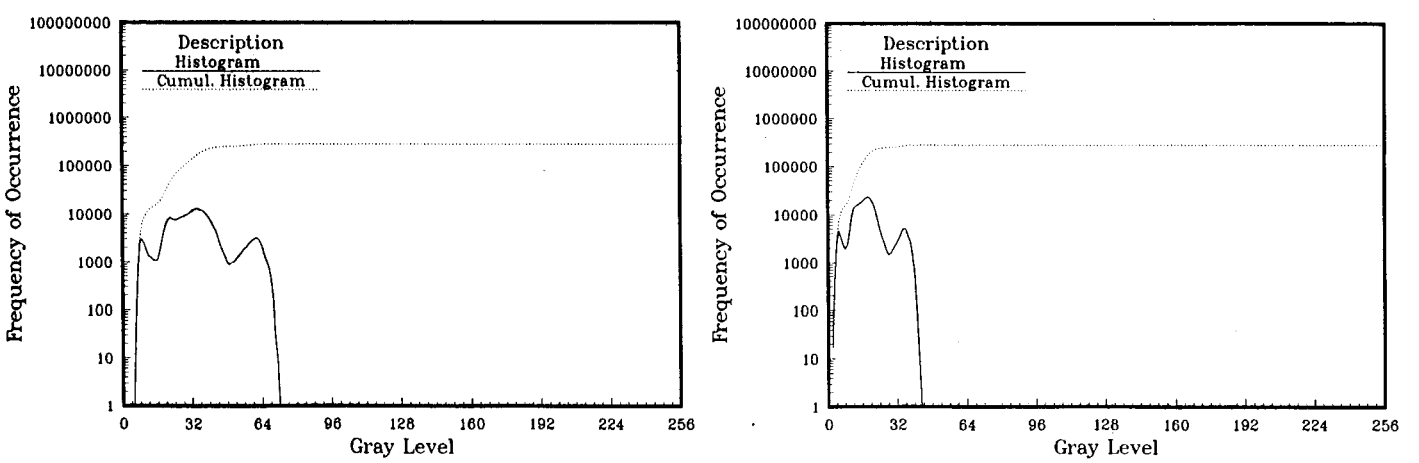

Figure 1b. Water vapor absorption channels at 0.94 μm and 1.14 μm.

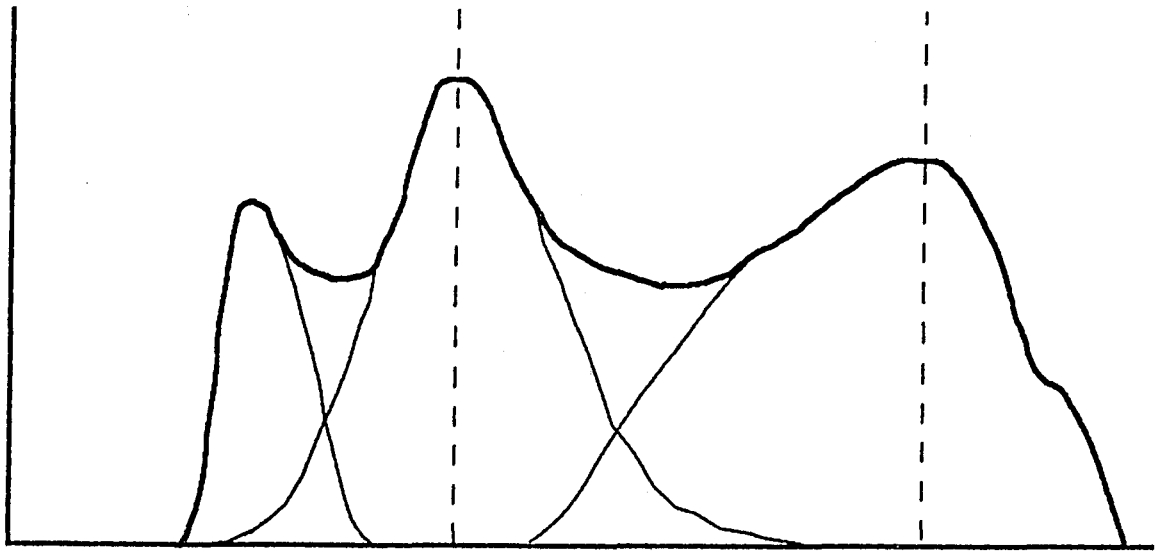

Figure 2. Typical histogram for an AVIRIS scene.

the composite envelope distribution being shifted to the lower albedo end. However, it is observed that the distribution of different classes is shifted by a different degree. These effects can be explained by the attenuation of radiation by water vapor. Since clouds are higher objects and the upper atmosphere has substantially lower humidity, the attenuation of the radiation reflected by clouds is much less than that reflected by background. Table 1 shows the 3-band ratios of the second and third maxima for scene AS0628. The 3-band ratio of the first maximum is not compared since this distribution is likely to be heavily contaminated by the left tail of the second distribution (Fig. 2).

Table 1. Ratios at the 2nd and 3rd maxima of the histograms for different scenes.

	Ratio at Maximum		Cloud Cover
Scene	second	third	%
AS0526	0.32	0.39	30.9
AS0590	0.51	*	17.8
AS0628	0.25	0.29	33.1
AS0630	0.37	*	5.1

*No third maximum for the scene due to low cloud cover

After the observation and reasoning made above, we use the 3-band ratio of the background maximum as the lower limit in the 3-band process. The range of the 3-band ratios is thus reduced and the resulting image is further enhanced. The improvement can be seen in Figure 3 for scene AS0590. (Detail may be lost in reproduction.) We can therefore choose a threshold on this image with ease and filter out background before we color code the optical depths of clouds. Using the cutoff ratio, a cloud cover of 17.8% is found, which is higher than the 15+% obtained by the original method (Gao and Goetz, 1990a). Therefore more cloudy area is preserved.

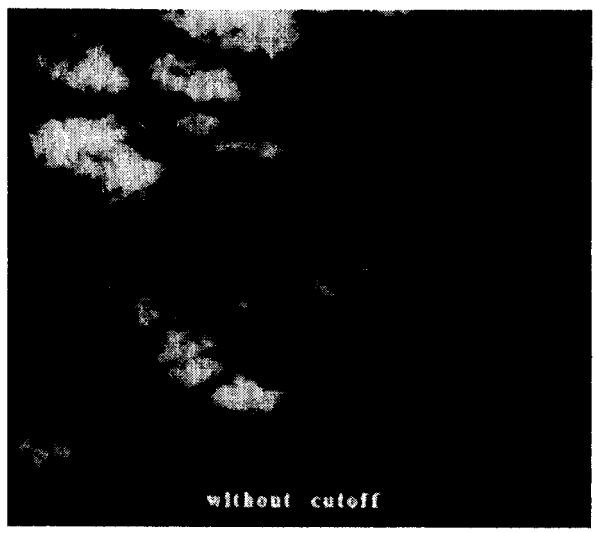

Figure 3a. Ratioed image for AS0590 without a cutoff ratio.

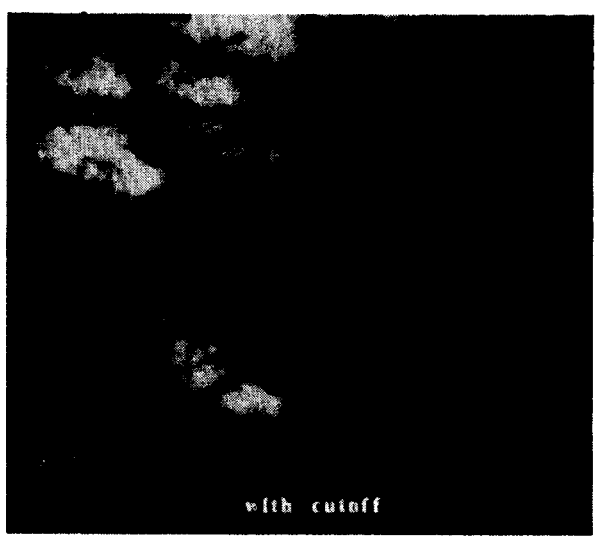

Figure 3b. Ratioed image for AS0590 with a cutoff ratio.

OPTICAL DEPTH RETRIEVAL

Model Description

A discrete ordinate radiative transfer model (Stamnes and Dale, 1981) is used to simulate the albedos being observed by the instrument under the same radiometry. In this preliminary study a uniform layer of cloud with certain optical depth is put in between two vacuum spaces. In other words there is no water vapor absorption or Rayleigh scattering effect simulated in the model. At the bottom of the lower space is a Lambertian surface with an albedo obtained by analyzing the histogram of the scene (i.e., the albedo corresponding to the background maximum). Figure 4 is a schematic diagram for the model setup.

Procedure and Results

Nakajima and King (1990) showed that at 0.752 μm the albedo is sensitive to optical thickness and insensitive to the droplet size distribution of the cloud. Therefore we chose to use the C1 size distribution from Diermendjian (1969) and ran a Mie scattering calculation at 0.752 μm to get the Lengendra polynomial expansion of the phase function, which is then fed to the radiative transfer model to calculate albedos for a set of optical thicknesses. We then used the calculated albedos to contour the optical thicknesses of the given scene. Then the scene was spatially degraded by averaging 24 x 24 pixels

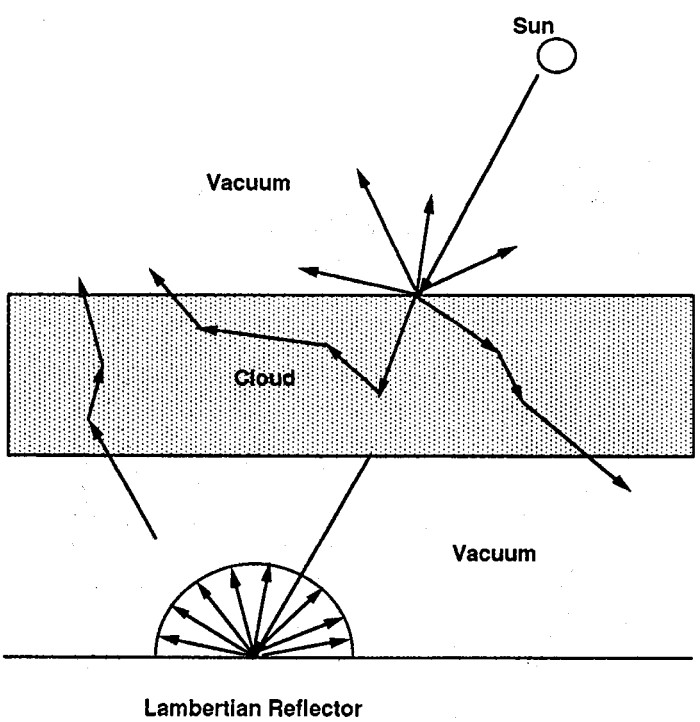

Figure 4. Schematic diagram of model setup.

(480 m x 480 m) on the original image to simulate the best resolution of MODIS-N (MODerate resolution Imaging Spectrometer-Nadir, another EOS facility instrument) data. A comparison of scene AS0526 is shown in Figure 5.

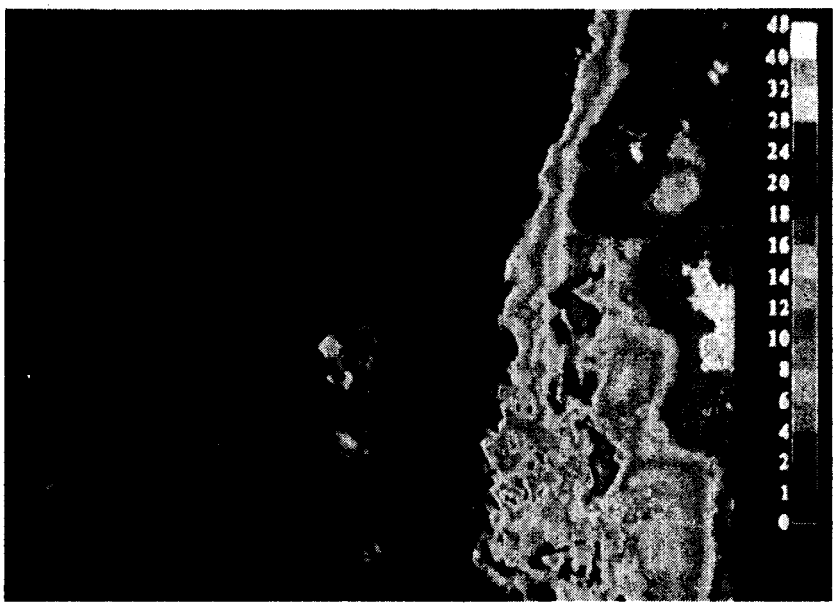

Figure 5a. Cloud optical thickness result with original resolution.

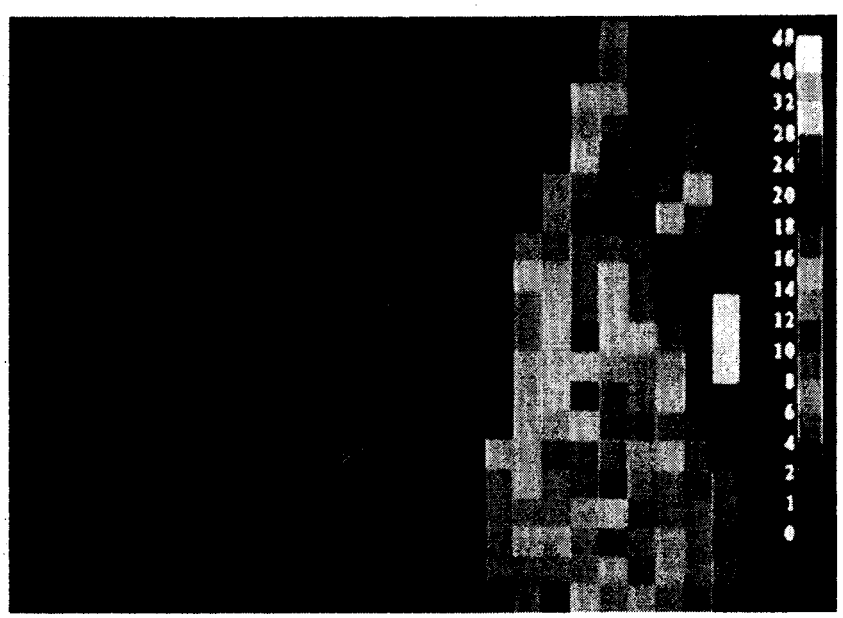

Figure 5b. Cloud optical thickness result with coarse resolution. (480 m x 480 m)

It can be seen that much of the detail of the fine distribution of the optical thickness is lost in the image with coarser resolution. Smaller clouds and optically thinner pixels disappeared in the averaging process which results in a decrease of cloud cover from 33.1% to 30.8%.

CONCLUSION

The original Gao and Goetz (1990a) technique in identifying cloudy areas is improved by using a lower limit of the ratio suggested by the background albedos in the 3-band ratioing process. A threshold can then be chosen without ambiguity to single out clouds from background. Then the images are contoured with varying optical thickness according to albedos resulting from radiative transfer model calculations. A comparison is made between images with original resolution and a 24 times lower resolution. A great loss in detail of the optical thickness distribution can be seen along with a lower cloud cover. Therefore it is concluded that a higher resolution data set is necessary to validate the lower resolution data which has the advantage of global coverage.

REFERENCE

Diermendjian, D., 1969. *Electromagnetic scattering on spherical polydispersions*. American Elservier Publishing Company, New York, 260pp.

Gao, B.-C., and A. F. H. Goetz, 1990a. Determination of cloud area from AVIRIS data. *Proceedings of 2nd AVIRIS workshop* (this JPL publication).

Gao, B.-C., and A. F. H. Goetz, 1990b. Column atmospheric water vapor and vegetation liquid water retrievals from airborne imaging spectrometer data *J. Geophys. Res.*, vol. 90, No. D4, 3549–3564.

Nakajima, N., and M. D. King, 1990. Determination of the optical thickness and effective particle radius of clouds from reflected solar radiation measurements. Part 1: theory. *J. Atmos. Sci.* (in press).

Parker, L., and B. A. Wielicki, 1989. Comparison of satellite-based cloud retrieval methods for cirrus and stratocumulus. FIRE Science Meeting, Monterey, California, U.S.A., July 10–14, pp 219–223.

Stamnes, K., and H. Dale, 1981. New look at the discrete ordinate method for radiative transfer calculations in anisotropically scattering atmospheres. Part 2: intensity computations. *J. Atmos. Sci.*, vol. 38, No. 12, 2696–2706.